Neuroepigenetics 6 (2016) 1–9

Contents lists available at ScienceDirect

Neuroepigenetics

journal homepage: www.elsevier.com/locate/nepig

Novel method to ascertain chromatin accessibility at specific genomic loci from frozen brain homogenates and laser capture microdissected defined cells

Elaine Delvaux [a,b], Diego Mastroeni [a,b,c], Jennifer Nolz [a,b], Paul D. Coleman [a,b,*]

[a] ASU-Banner Neurodegenerative Disease Research Center, Biodesign Institute and School of Life Sciences, Arizona State University, Tempe, AZ, USA
[b] L.J. Roberts Center for Alzheimer's Research, Banner Sun Health Research Institute, 10515 W Santa Fe Dr, Sun City, AZ 85351, USA
[c] Department of Psychiatry and Neuropsychology, School for Mental Health and Neuroscience (MHeNS), Faculty of Health, Medicine and Life Sciences, European Graduate School of Neuroscience (EURON), Maastricht University Medical Centre, Maastricht, the Netherlands

ARTICLE INFO

Article history:
Received 24 November 2015
Received in revised form 24 February 2016
Accepted 15 March 2016

Keywords:
Chromatin
qPCR
Benzonase

ABSTRACT

We describe a novel method for assessing the "open" or "closed" state of chromatin at selected locations within the genome. This method combines the use of Benzonase, which can digest DNA in the presence of actin, with quantitative polymerase chain reaction to define digested regions. We demonstrate the application of this method in brain homogenates and laser captured cells. We also demonstrate application to selected sites within more than 1 gene and multiple sites within 1 gene. We demonstrate the validity of the method by treating cells with valproate, known to render chromatin more permissive, and by comparison with classical digestion with DNase I in an in vitro preparation. Although we demonstrate the use of this method in brain tissue, we also recognize its applicability to other tissue types.

1. Introduction

The epigenetic regulation of chromatin structure is a major component of the gene expression regulatory machinery, and this regulation is accomplished by multiple mechanisms including DNA methylation and hydroxymethylation, multiple histone modifications, binding molecules, and complex interactions among all these elements (Jaenisch and Bird, 2003; Mastroeni et al., 2011; Chouliaras et al., 2013). These complex interactions converge to modulate chromatin structure, much as multiple inputs converge on the final common path of the anterior horn cells (Sherrington, 1906). By analogy, we posit chromatin structure as the final common path of multiple epigenetic mechanisms.

Chromatin structure determines whether any selected segment of DNA is accessible to transcription factors, DNA binding proteins, or other modifiers which govern a gene's availability for transcription (Quina et al., 2006). There are multiple classes of methods for examining chromatin structure. Broadly speaking, these are methods that use DNase I digestion, chromatin precipitation, matrix-assisted reader chromatin capture, and others, which are typically followed by methods to determine location of permissive or repressive chromatin structure.

In the past, permissive, or open, chromatin has been identified by DNase I nuclease sensitivity analysis (Krebs and Peterson, 2000), and more recently, open chromatin data generated from DNase-seq have been able to predict cell-type–specific gene expression (Natarajan et al., 2012).

An overview of current methods available to ascertain chromatin structure yields a broad range of approaches, many of which are variations of chromatin immunoprecipitation (ChIP), an antibody-based methodology first described by Gilmour and Lis (1984, 1985). Fast carrier ChIP (Fast CChIP) can be used to study transcription factor binding in small amounts of fresh tissue (Hao et al., 2008). Another ChIP-based technique uses genomewide chromatin immunoprecipitation in concert with tiling microarrays (ChIP-chip). ChIP-chip, along with ChIP–quantitative polymerase chain reaction (qPCR), showed that transcription factor FoxA1 is differentially recruited to cell-type–specific enhancers (Lupien et al., 2008). ChIA-PET combines ChIP with paired-end DNA sequencing to determine global de novo chromatin interactions (Fullwood et al., 2009). PAT-ChIP, also a ChIP-directed technique, was used to isolate, extract, and sequence chromatin from formalin-fixed, paraffin-embedded tissue samples (Fanelli et al., 2010; Fanelli et al., 2011; Amatori et al., 2014). A common method used to determine chromatin structure is DNase I digestion of DNA with subsequent sequencing of resulting fragments (DNase-seq).

* Corresponding author at: ASU-Banner Neurodegenerative Disease Research Center, Biodesign Institute and School of Life Sciences, Arizona State University, Tempe, AZ, USA.
E-mail address: paul.coleman@asu.edu (P.D. Coleman).

http://dx.doi.org/10.1016/j.nepig.2016.03.001

The sites of cleavage are called *DNase I hypersensitive sites* (DHSs), suggesting areas of the chromatin accessible to DNase digestion to be "open" and poised for transcription. A recent international epigenetic collaborative study, Encyclopedia of DNA Elements (ENCODE), created a genomewide map of DHSs in 125 human cell lines and tissue types and correlated those sites with ChIP-seq data (Thurman et al., 2012). In addition to genomewide mapping of DHS, DNase I sensitivity and sequencing can be used to analyze receptor binding influences on chromatin structure at specific gene loci in vitro (Tewari, et al., 2012). More recently, a modification to ChIP-Seq, called *Bar-ChIP*, allowed multiple DNA-protein interactions to be simultaneously profiled by attaching molecular barcodes to chromatin fragments from *Saccharomyces cerevisiae* (Chabbert et al., 2015).

Chromosome conformation capture (3C) technologies have been used for more than a decade. First described in Dekker et al. (2002), 3C delivers 3-dimensional chromatin structure information based on interaction frequencies between genomic loci. Some 3C technologies, such as e4C, use ChIP within the protocol (Sexton et al., 2012). Capture-C, the most recent derivative of the 3C technique, modifies the 3C method into a multiplexed, high-throughput approach to analyzing *cis*-acting elements that control gene expression (Hughes et al., 2014).

A ChIP-less technique to examine the epigenome, called *MARCC* (matrix-assisted reader chromatin capture), is a platform that probes combinatorial histone modification patterns to determine functional chromatin conformation (Su et al., 2014). Finally, direct chromatin PCR is a method for gene-specific chromatin analysis performed on cultured cells using properties of standard PCR buffers and thermal cycling temperatures to amplify open regions of chromatin (Vatolin, et al., 2012).

Although ChIP and non–ChIP-based techniques have been broadly used in elucidating chromatin structure and its impact on gene regulation, caveats to their use exist. The ChIP-based techniques rely on antibodies, which involve problems with antibody specificity and optimization (Orlando, 2000). Moreover, most ChIP and non–ChIP-based methods need large amounts of cultured cells or fresh tissue to start with. In addition, these complicated protocols take several days to complete and can be expensive with labor, reagents, equipment, and per-sample core costs (Sheffield and Furey, 2012).

A major limitation of DNase I–based methods is the susceptibility of DNase I to inhibition by actin, a component of many cells and tissues. Recently, a protocol was developed for determining chromatin accessibility in frozen tissue homogenates using Benzonase, a robust nuclease whose efficacy is not affected by the presence of actin (Grøntved et al., 2012). Here we describe a protocol to assess chromatin structure at specific loci using Benzonase digestion and qPCR of DNA extracted from frozen tissue homogenates and laser capture dissected defined cells. This protocol is relatively quick, inexpensive, and achievable in any research laboratory outfitted with standard real-time PCR equipment. This novel method will allow a more focused examination of chromatin structure, its influence on gene expression, and the impact it may have on gene expression in normal and diseased brain as well as other tissues.

2. Materials and methods

2.1. Tissue (samples)

All frozen brain tissue samples and frozen brain sections were obtained from the Brain Bank at Banner Sun Health Research Institute. Average postmortem delay at this Brain Bank is 2.6 hours. Homogenate studies used approximately 1 g of middle temporal gyrus (MTG) and cerebellum (CBL) from each of 3 nondemented controls (NDs) and 3 Alzheimer's disease (AD) cases. Laser capture microdissection (LCM) studies used 10-μm serial sections of MTG (area 22) from 1 ND and 1 AD case and 10-μm serial sections of hippocampus from 5 ND and 5 AD cases.

2.2. Primers

2.2.1. Primer design for chromatin accessibility analysis

Primers for KAT6B, APP, and RSP28 were designed to cover the area 300 base pairs (bp) upstream of the transcription start site and 100 bp downstream of the transcription start site. The primer sequences for GAPDH, CTCF4, and CTCF10 were taken from He et al. (2014) and chosen to represent areas of the genome known to be constitutively open (GAPDH) and/or uniform in openness across sample types (CTCF4, CTCF10) (Li et al., 2013). All primers were checked for specificity via the National Center for Biotechnology Information's BLAST search.

To examine chromatin structure in multiple regions of 1 gene, primers for ARC were designed based on ENCODE data (Thurman et al., 2012). ARC1 was located in the promoter region, an area identified with high significance as open chromatin and validated by DNase I hypersensitivity and formaldehyde-assisted isolation of regulatory elements (FAIRE) assays. This area contained DNase I hypersensitivity in 113 of 125 cell lines/types. Transcription factor ChIP-seq data show it to be densely populated with DNA binding proteins (transcription factors, transcription machinery components, chromatin factors) with varying degrees of occupancy. ARC2 was located adjacent to ARC1, breaching the start of the coding sequence. This area was validated by both DNase I hypersensitivity and FAIRE assays with DNase I hypersensitivity in 16 of 125 cell lines/types. ChIP-seq data identified several DNA binding proteins with varying degrees of occupancy. ARC3 was located near the end of the gene in the third exon. This area contained DNase I hypersensitivity in 10 of 125 cell lines/types. This region was considered high significance as open chromatin but not validated by both DNase I and FAIRE assays. Transcription factor CTCF occupancy is shown to be weak. ARC4 was designed in an area that could be considered a "control," an intronic region between exons 2 and 3.

To determine the optimal annealing/extension temperatures for all primer sets designed, a gradient PCR with melting curve was run. Based on the results of the gradient, a standard curve PCR was performed to test the PCR efficiency. Efficiency greater than 90% was acceptable. After optimizing PCR protocols, the samples were run within those parameters. Primer sequences are found in Table 1.

2.3. Brain homogenates

2.3.1. Benzonase digestion (adapted from Grøntved et al., 2012)

Approximately 600 mg of frozen brain tissue was pulverized with a mortar and pestle that had been prechilled on dry ice. The pulverized tissue was transferred to a prechilled 15-mL tube and then suspended in 4 mL of lysis buffer (30 mmol/L Tris-HCL [pH 8.0], 2 mmol/L EDTA, 2 mmol/L EGTA, 20 mmol/L sodium butyrate, 2 mmol/L sodium orthovanadate, 4 mmol/L sodium fluoride, protease

Table 1
Primer sequences used for qPCR to determine chromatin accessibility

Gene	Forward	Reverse
KAT6B	CCCCAATGGGCTGCAGAGTGGTTAG	CGCTGCCGCTGCCTGAGAAACT
APP	CTCCCACTGTTCACGAAGCCCAGGT	CTACCGCTGCCGAGGAAACTGACG
ARC1	GGGCCTCGCTGGCTGCATAAAGAG	GTCCGGTGGTCCAGCTCCATCTGT
ARC2	ACTCGCAGCGCTGGAAGAAGTCCAT	GCGTAGGGGCTGACGGTGTAGTCGT
ARC3	TGGTCCTTCACTGCCCACTCTCCTG	CTAAGCTGGGGCTCCTGCCCTCTG
ARC4	ATGAGCTCCTCCCCAGACCCCAGAC	GCAGTGAAGGACCACGCAGGACAGT
RPS28	AGAGCGAAGGGTCCCGGCTTAGGAG	AGAGGAGTCACGTGCTTCGGGGAGA
GAPDH	AAAAGCGGGGAGAAAGTAGG	AGAGGAGTCACGTGCTTCGGGGAGA
CTCF4	CCCCAGAGAGTAGGGAACAG	GGCACGCAAAGACATACTGA
CTCF10	AGAGCACCCCCTACTGGCTAA	TAAGAAGCTGTGCGCGATGAC

inhibitor cocktail [Pierce]) using a syringe fitted with a 20-gauge needle. Volume was brought up to 6 mL with lysis buffer. Using a 23-gauge needle, the suspension was mixed and distributed in 500-μL equal-volume aliquots into 2-mL microfuge tubes and incubated on ice for 5 minutes. Aliquots not needed were frozen at 20°C for later use. To the aliquots being used, 500 μL of nuclease digestion buffer (30 mmol/L Tris-HCL [pH 8.0], 14 mmol/L $MgCl_2$, 0.5% NP-40, 0.2% fatty acid–free bovine serum albumin, 0.25 U/μL Benzonase [EMD Millipore]) was added. A no-nuclease control sample was also prepared. The tubes were gently inverted to mix and incubated at 37°C for 3 minutes. Immediately after the incubation, EDTA (at 50-mmol/L final concentration) and sodium dodecyl sulfate (SDS) (at 0.1% final concentration) were added to stop the digestion reaction. Fifty microliters of RNaseA/RNaseT1 (Ambion/Life Technologies) was added and incubated overnight at 45°C. After incubation, SDS was added to final concentration of 0.75% and placed at 45°C for 2 hours. Proteinase K (Sigma) was then added to final concentration of 0.8 μg/mL and incubated overnight at 45°C. Digested and undigested DNA reactions were purified by gel extraction (Wizard SV Gel and PCR Clean Up, Promega) or phenol chloroform extraction and ethanol precipitation and then quantified with Quant-iT PicoGreen Assay (Life Technologies).

2.3.2. Chromatin accessibility analysis by qPCR (adapted from Rao et al., 2001)

Five nanograms of digested and undigested DNA from each sample was amplified in triplicate for 50 cycles on an iCycler iQ (Bio-Rad) using EpiQ SYBR Green Supermix (Bio-Rad) (This supermix was discontinued in early stages of protocol design. iTaq Universal SYBR Green Supermix [Bio-Rad] was used for remaining experiments.) and 2-μmol/L primers under the optimized parameters for each primer set. In the resulting PCR analyses, higher C_T values indicate more "open" chromatin accessible to regulatory elements.

2.4. Laser capture microdissected derived cells

2.4.1. Benzonase digestion of many cells

Ten-micrometer frozen sections of hippocampus from (5) AD and (5) ND cases were mounted on PEN slides (Leica) and kept under desiccant at −80°C until use. After a brief thaw, sections were placed in 100% EtOH then 95% EtOH and a final 70% ethanol for 5 seconds each then rinsed with molecular grade water. Neutral red stain (1%) was applied for 30 seconds and then rinsed twice with molecular grade water and dehydrated for 5 seconds in 70% EtOH then 95% EtOH and for 1 minute in 100% ethanol. Laser capture microdissection of dentate gyrus granule cells was performed on an LMD 6500 (Leica). Briefly, 40 μL of lysis buffer (20 mmol/L Tris-HCL [pH 7.5], 2 mmol/L EDTA, 1 mmol/L EGTA, 0.5% glycerol, 20 mmol/L sodium butyrate, 2 mmol/L sodium orthovanadate, 4 mmol/L sodium fluoride, protease inhibitor cocktail [Pierce]) was added to the cap of the tube where the sample was captured. After a 1-minute spin, another 40 μL of lysis buffer was added to the cap. The tube was set upside down on a bench for 20 minutes, spun down in a bench top centrifuge for 1 minute, and then split equally (40 μL) into 2 tubes for no-enzyme control and enzyme digestion. For enzyme digestion, 40-μL nuclease digestion buffer (40 mmol/L Tris-HCL [pH 8.0], 6 mmol/L $MgCl_2$, 0.3% NP-40, 1% glycerol, 0.25 U/μL Benzonase [EMD Millipore]) was added. The no-nuclease control tube received 40 μL of nuclease digestion buffer minus the Benzonase. Both tubes were placed at 37°C for 2.5 minutes. To stop the reaction, EDTA (10 mmol/L final) and SDS (0.75% final) were added to each tube. Then, 4 μL RNaseA/RNase T1 was added, and the tubes were placed at 45°C overnight. The next day, SDS at 0.75% final concentration was added and incubated for 2 hours at 45°C. Next, Proteinase K (0.5 μg/mL final) was added and incubated overnight at 45°C. The digested and undigested DNA reactions were purified by phenol chloroform extraction and ethanol precipitation.

2.4.2. Chromatin accessibility analysis by qPCR of many cells (dentate gyrus granule cells)

Digested and undigested DNA from each sample was amplified in duplicate for 50 cycles on an iCycler iQ (Bio-Rad) using iTaq Universal SYBR Green Supermix (Bio-Rad) and 2-μmol/L primers under the optimized parameters for each primer set.

2.4.3. Benzonase digestion of few cells

Ten-micrometer frozen serial sections of MTG from (1) AD and (1) ND case were mounted on PEN slides (Leica) and kept under desiccant at −80°C until use. After brief thaw, sections were stained with 1% neutral red to identify pyramidal neurons. Neurofibrillary tangle-bearing neurons were identified by staining an adjacent section with 0.1% Thioflavin S for 15 seconds. Non–tangle-bearing pyramidal neurons were chosen after comparing the adjacent sections and excluding tangle-bearing cells. Laser capture microdissection of nontangle neurons was performed on a PALM MicroBeam (Zeiss) where approximately 50 cells were captured into AdhesiveCap tubes (Zeiss). Twenty microliters of lysis buffer (20 mmol/L Tris-HCL [pH 7.5], 2 mmol/L EDTA, 1 mmol/L EGTA, 0.5% glycerol, 20 mmol/L sodium butyrate, 2 mmol/L sodium orthovanadate, 4 mmol/L sodium fluoride, HALT protease inhibitor cocktail [Pierce]) was added to the cap of the tube. The tube was set upside down on a bench for 20 minutes and then spun down in a bench top centrifuge for 1 minute. An additional 10 μL of lysis buffer was added to the tube and then split equally (~15 μL) into 2 tubes for no-enzyme control and enzyme digestion. For enzyme digestion, 15-μL nuclease digestion buffer (40 mmol/L Tris-HCL [pH 8.0], 6 mmol/L $MgCl_2$, 0.3% NP-40, 1% glycerol, 0.25 U/μL Benzonase [EMD Millipore]) was added. The no-nuclease control tube received 15 μL of nuclease digestion buffer minus the Benzonase. Both tubes were placed at 37°C for 2.5 minutes. To stop the reaction, EDTA (10 mmol/L final) and SDS (0.75% final) were added to each tube. Then, 1.5 μL RNaseA/RNase T1 was added, and the tubes were placed at 45°C overnight. The next day, SDS at 0.75% final concentration was added and incubated for 2 hours at 45°C. Next, Proteinase K (0.5 μg/mL final) was added and incubated overnight at 45°C. The digested and undigested DNA reactions were purified by phenol chloroform extraction and ethanol precipitation.

2.4.4. Chromatin accessibility analysis by qPCR of few cells (non–tangle-bearing neurons)

Approximate equivalents of 5 cells underwent qPCR on an iCycler iQ (Bio-Rad) with the same APP primers and conditions as with frozen homogenates protocol except that the cycle number was extended to 80 cycles because of the minute amount of starting material. A 1.5% agarose gel was run to verify amplification of 260-bp amplicon (data not shown).

2.5. Validation in vitro by treatment of cells with a reagent known to lead to open, permissive chromatin

2.5.1. Valproic acid treatment to decondense chromatin in SH-SY5Y cells

SH-SY5Y neuroblastoma cells (ATCC) were cultured and maintained in a humidified 37°C incubator with 5% CO_2 in complete Dulbecco modified Eagle medium (DMEM) (DMEM with high glucose [Life Technologies], 10% fetal bovine serum [Gemini Bio-Products], 2% HEPES [Irvine Scientific], 1% sodium pyruvate [Thermo Scientific], 1% penicillin/streptomycin [Life Technologies], and 0.1% gentamycin [Life Technologies]). After 4 days in culture, cells were seeded at a density of 2.6×10^5 cells/mL in 6-well plates. Two days later, they were fed with complete DMEM, and half the wells were treated with 1 mmol/L valproic acid (VPA) (Sigma), an HDAC inhibitor known to decondense chromatin (Felisbino et al., 2011; Felisbino et al., 2014), and half were left untreated. After incubating for 24 hours at 37°C and 5% CO_2, they were washed twice in 1× phosphate-buffered saline, collected by centrifugation, washed twice in ice-cold wash buffer (20 mmol/L

Tris-HCL [pH 7.5], 137 mmol/L NaCl, 1 mmol/L EDTA, 10 mmol/L sodium butyrate, 10 mmol/L sodium orthovanadate, 2 mmol/L sodium fluoride, 1 × HALT protease inhibitor cocktail [Pierce]), and resuspended in 1-mL lysis buffer (20 mmol/L Tris-HCl [pH 7.5], 2 mmol/L EDTA, 1 mmol/L EGTA, 20 mmol/L sodium butyrate, 2 mmol/L sodium orthovanadate, 4 mmol/L sodium fluoride, 0.5% glycerol, and 1 × HALT protease inhibitor cocktail [Pierce]) and aliquot 500 μL to 2 tubes, one for enzyme digestion and one no-enzyme control. Next, Five hundred microliters of nuclease digestion buffer (40 mmol/L Tris-HCl [pH 8.0], 6 mmol/L $MgCl_2$, 0.3% NP-40, and 1% glycerol) was added to each tube. Benzonase was added to appropriate tubes for a final concentration of 0.5 U/mL. Tubes were incubated at 37°C for 3 minutes. To stop the reaction, EDTA (10 mmol/L final) and SDS (0.75% final) were added to each tube. Next, Proteinase K (0.5 μg/mL final) was added and incubated overnight at 45°C. The digested and undigested DNA reactions were purified by phenol chloroform extraction and ethanol precipitation and quantified by Quant-iT PicoGreen Assay (Life Technologies). Digested and undigested DNA (5 ng) from each sample was amplified in duplicate on an iCycler iQ (Bio-Rad) using iTaq Universal SYBR Green Supermix (Bio-Rad) and 2-μmol/L primers as per the optimized parameters determined by gradient and melting curve PCR.

2.6. Validation in vitro by comparison of Benzonase with DNase I digestion in SH-SY5Y cells

SH-SY5Y cells were cultured and maintained as described above. Four concentrations of Benzonase (none, 0.33 U, 1 U, 3 U) were used to digest 3.4×10^6 cells as detailed above. The DNase I digestion protocol was based on Song and Crawford (2010). For DNase I digestion, 3.7×10^7 cells were pelleted in a 15-mL tube and then resuspended by gentle flicking in 1 mL ice-cold resuspension buffer (RSB) (10 mmol/L Tris-HCl [pH 7.4], 10 mmol/L NaCl, 3 mmol/L $MgCl_2$). Lysis buffer (RSB + 0.1% IGEPAL CA-630 [Sigma]) was poured slowly into the tube and then centrifuged (500*g*) at 4°C for 10 minutes. Supernatant was completely removed, and nuclei were resuspended in 600 μL of cold RSB by gentle flicking. The nuclei were aliquoted equally into 5 microfuge tubes containing different concentrations of DNase I (Sigma) (none, 0.12 U, 0.4 U, 1.2 U, 4 U). Tubes were incubated at 37°C for 11 minutes. To stop the reaction, 160 μL of 50 mmol/L EDTA was added, and tubes were inverted 5 times to mix. The digested and undigested DNA reactions were purified by phenol chloroform extraction and ethanol precipitation and quantified by Quant-iT PicoGreen Assay (Life Technologies). Digested and undigested DNA (5 ng) from each sample was amplified in duplicate on an iCycler iQ (Bio-Rad) using iTaq Universal SYBR Green Supermix (Bio-Rad) and 2-μmol/L primers as per the optimized parameters determined by gradient and melting curve PCR.

3. Results

3.1. Homogenate samples

3.1.1. 1 case of AD, promoter region of 2 genes in 2 different brain regions

For proof of concept, brain homogenates from MTG and CBL of 1 AD case were digested with Benzonase. The amplification curves of the digested and undigested samples for genes KAT6B and APP demonstrate that undigested DNA has the lowest C_T values for both genes and brain regions, and the promoter regions of KAT6B and APP are more open in MTG than CBL (Fig. 1). APP plays a prominent role in Alzheimer's pathology, and increased expression of KAT6B, a lysine acetyltransferase, has been associated with decreased expression of synaptophysin, a presynaptic molecule. Because the MTG is more affected in AD than is the CBL, it can be expected that the promoter regions of these genes would be more permissive in the MTG, consistent with literature showing CBL to be less affected than MTG in Alzheimer's disease.

3.1.2. More cases and 2 brain regions with comparison of Alzheimer's and control samples

Subsequently, the number of cases was increased to MTG and CBL of 3 ND and 3 AD cases. In MTG, KAT6B and APP were more open in AD than ND (Fig. 2A). The results also showed that in CBL, KAT6B and APP were more open in AD as compared with ND (Fig. 2B), suggesting some effect of AD in CBL, although less than in MTG, replicating the conclusion from Fig. 1 that MTG is more affected than CBL (compare relative heights of bars in Fig. 2A, temporal gyrus, and 2B, CBL). C_T values indicate that both genes are more open in MTG (Fig. 2A) than in CBL (Fig. 2B).

3.1.3. More regions within 1 gene—homogenates of MTG

Up to this point, chromatin accessibility analysis was limited to the promoter region of genes. To demonstrate ability to examine multiple regions within 1 gene, primers were designed for 4 regions of the Arc gene. Arc was selected for study because of its role as an immediate early gene important for memory (Guzowski et al., 2000). Four regions within the Arc sequence were chosen based on DNase I sensitive sites and $H_3K_4Me_3$ ChIP analysis from the ENCODE project (Thurman et al., 2012). In this brain region, analysis of variance (ANOVA) shows differential relative openness among the 4 arc regions examined ($P = 0.01$). The promoter region of Arc (ARC1) is significantly less open in AD than in ND (t test $P < .05$) (Fig. 3), consistent with the deficient memory function characteristic of Alzheimer's disease.

3.2. Laser capture samples

3.2.1. Many dentate gyrus granule cells

To test compatibility of our protocol with LCM, we used a Leica LMD 6500 to dissect a portion of the dentate gyrus granule cell layer followed by Benzonase digestion and qPCR for 4 regions of the ARC gene. Fig. 4 shows representative qPCR traces of the promoter region of ARC from 1 ND and 1 AD case (Fig. 4A) and of an intronic region of ARC in 1 ND and 1 AD case (Fig. 4B). The C_T values of all undigested samples are comparable and lower than digested samples, as expected. ANOVA analysis of the C_T values showed no significant difference between primer groups and no significant difference in openness between ND and AD in any of the gene regions (t test) (Fig. 5). For example, in support of this analysis seen in Fig. 4B, the qPCR traces of ARC4 in digested ND and AD samples show that chromatin appears to be equally accessible. This result differs from the result shown for homogenate data in Fig. 3. We emphasize that this is a different brain region in which neurons do not typically show the neurofibrillary tangle pathology of Alzheimer's disease and granule cells of the dentate gyrus are not lost in AD (West et al., 1994).

3.2.2. Few MTG pyramidal neurons

To test the lower limit of the protocol, layer 3 pyramidal neurons from 1 ND and 1 AD case with no tangle pathology were selected in MTG and captured via LCM. Samples equaling 5 cell equivalents were subjected to Benzonase digestion and chromatin accessibility for APP determined by PCR. The data indicate that the promoter region of the APP gene is less open in AD than in NDs (Fig. 6). A 1% agarose gel indicated PCR products at the appropriate size (data not shown). These data indicate that this protocol can be used on as few as 5 laser captured cells but appear contradictory to the homogenate data. We can theorize as to why the difference in results, from the heterogeneity of cells in homogenates masking the data (Wills et al., 2013) to the minute starting material from single cells confounding the data. Nevertheless, we assert that without additional samples and

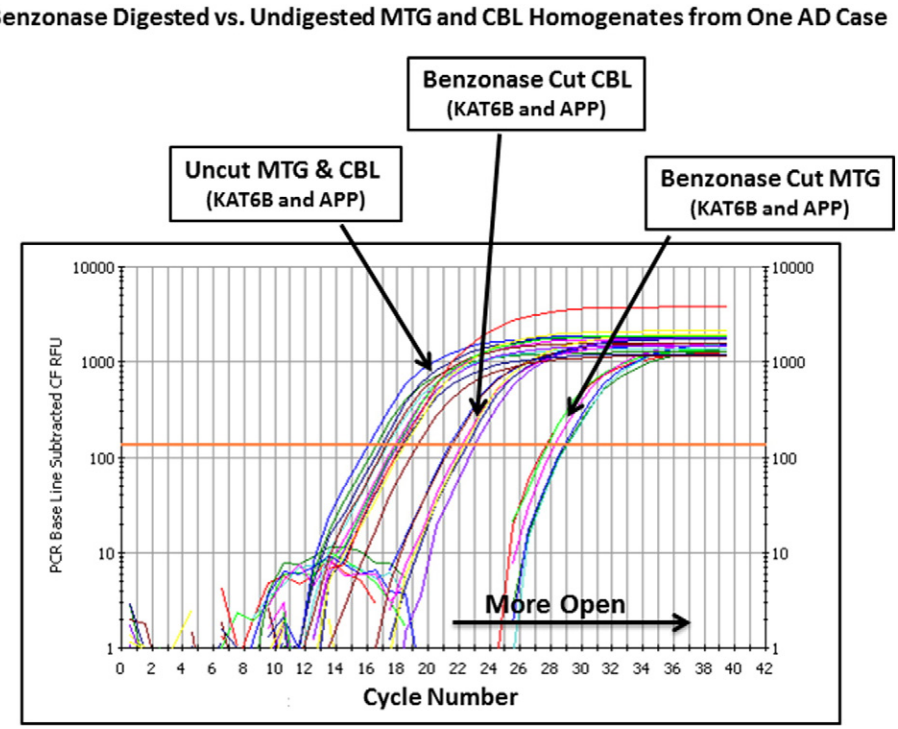

Fig. 1. MTG and CBL homogenates of frozen tissue from 1 AD case underwent Benzonase digestion then qPCR to determine relative openness of chromatin in the promoter region of APP and KAT6B. qPCR traces show that the promoter regions of KAT6B and APP appear to be more accessible in MTG than in CBL. The lower C_T values of the uncut samples are consistent with intact/undigested DNA.

replicates, we cannot make a determination of chromatin accessibility of APP in ND or AD in non–tangle-bearing neurons of the MTG.

3.3. Validation

3.3.1. By treatment known to open chromatin

We treated SH-SY5Y cells with VPA, an HDAC inhibitor known to decondense chromatin (Marchion et al., 2005). The prediction was that VPA-treated cells would show more open chromatin than cells not treated with VPA. Fig. 7 shows this to be true for the promoter region of KAT6B and APP genes, with equivocal results in the promoter region of Arc (ARC1) (Fig. 7). The lack of effect that VPA had on Arc could be inherent to SH-SY5Y cells. Past studies found that Arc expression in these cells is a fine-tuned balancing act between translation-dependent mRNA decay and proteasomal degradation, and without specific stimulation, Arc expression is negligible (Soulé et al., 2012). This leads us to consider that regulation of Arc may not be so dependent on histone acetylation; thus, VPA may not act on the chromatin in the promoter region of Arc the same way as with KAT6B and APP.

The results of the chromatin accessibility analysis showed no difference in relative openness in the no-Benzonase digestion in VPA-treated and untreated cells but large increases in openness in VPA-treated cells digested with Benzonase, as expected (Fig. 7). In addition, it appeared that the VPA relaxed the chromatin in the primer-specific areas of KAT6B and APP, with a significant difference in relative openness between VPA treated without Benzonase digestion and VPA treated plus Benzonase digestion with Student t test of $P < .05$ (Fig. 7).

3.3.2. By comparison with DNase I

To further validate our Benzonase protocol, we compared it with conventional DNase I digestion, the standard method for determining active, or "open," areas of chromatin (Krebs and Peterson, 2000).

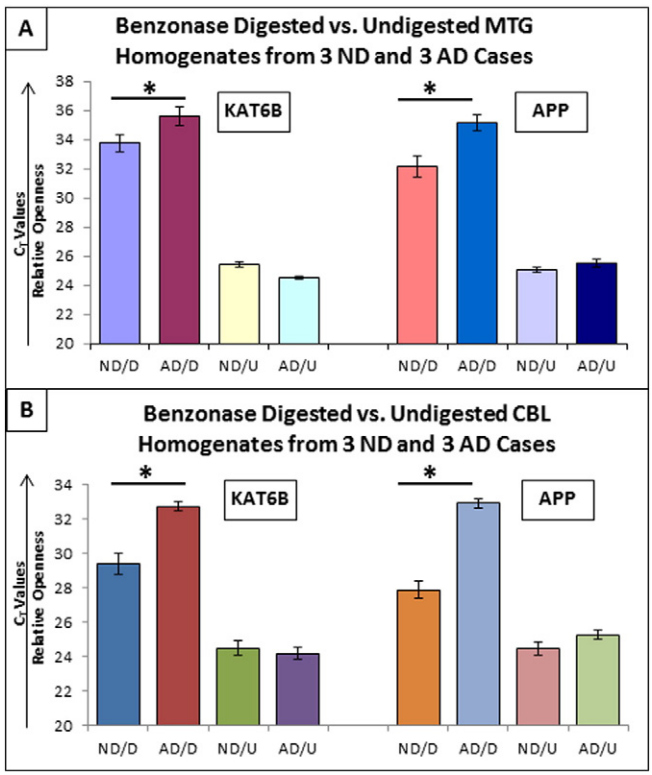

Fig. 2. MTG and CBL homogenates of frozen tissue from 3 ND and 3 AD cases underwent Benzonase digestion then qPCR to determine relative openness of chromatin in the promoter region of APP and KAT6B. (A) In MTG, promoter regions of KAT6B and APP appear to be more open in AD than ND. *Student t test $P < .05$. (B) In CBL, promoter regions of KAT6B and APP appear to be more open in AD than ND. *Student t test $P < .05$. Abbreviations: D, Benzonase digested; U, undigested. Error bars signify SEM.

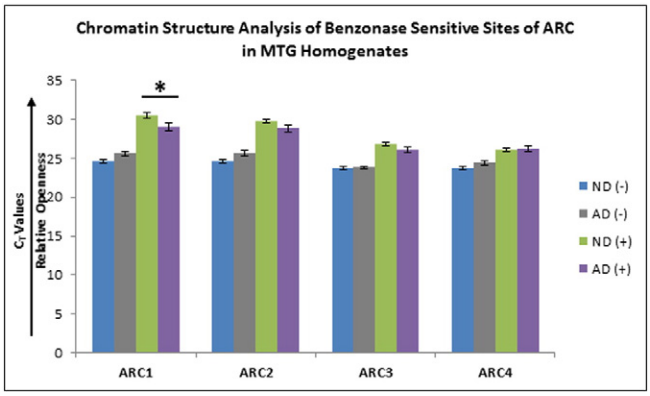

Fig. 3. MTG homogenates from 3 ND and 3 AD cases underwent Benzonase digestion and qPCR. Four regions of the ARC gene were examined for chromatin accessibility. ANOVA between primer groups was $P = 0.01$. *Student t test ($P < .05$) showed that AD is significantly less open than ND in the promoter region of the gene (ARC1). Abbreviations: ND (−), nondemented control undigested; AD (−), Alzheimer's disease undigested; ND (+), nondemented control Benzonase digested; AD (+), Alzheimer's disease Benzonase digested. Error bars signify SEM.

To compare Benzonase digestion to DNase I digestion, we analyzed chromatin accessibility in 7 distinct regions of the genome after digesting SH-SY5Y cells with selected concentrations of each enzyme. Comparison of the peaks in the Benzonase-digested cells (Fig. 8A) to those in the DNase I–digested cells (Fig. 8B) showed similar patterns of relative openness, substantiating that the 2 enzymes function comparably. To determine the effect of concentration of DNase I and Benzonase on our data, we converted the data to standard scores. The resulting standard scores are presented in Fig. 8C, which indicates that under the conditions examined and over the concentration ranges used, Benzonase and DNase I act very similarly.

4. Discussion

We have described a new method for examining chromatin structure that digests DNA with Benzonase to avoid the problems posed by actin when using DNase I. We have demonstrated the application of this method to homogenates of brain tissue, to laser microdissected brain tissue, to small numbers of neurons obtained by LCM, and to in vitro cell preparations. We have demonstrated the

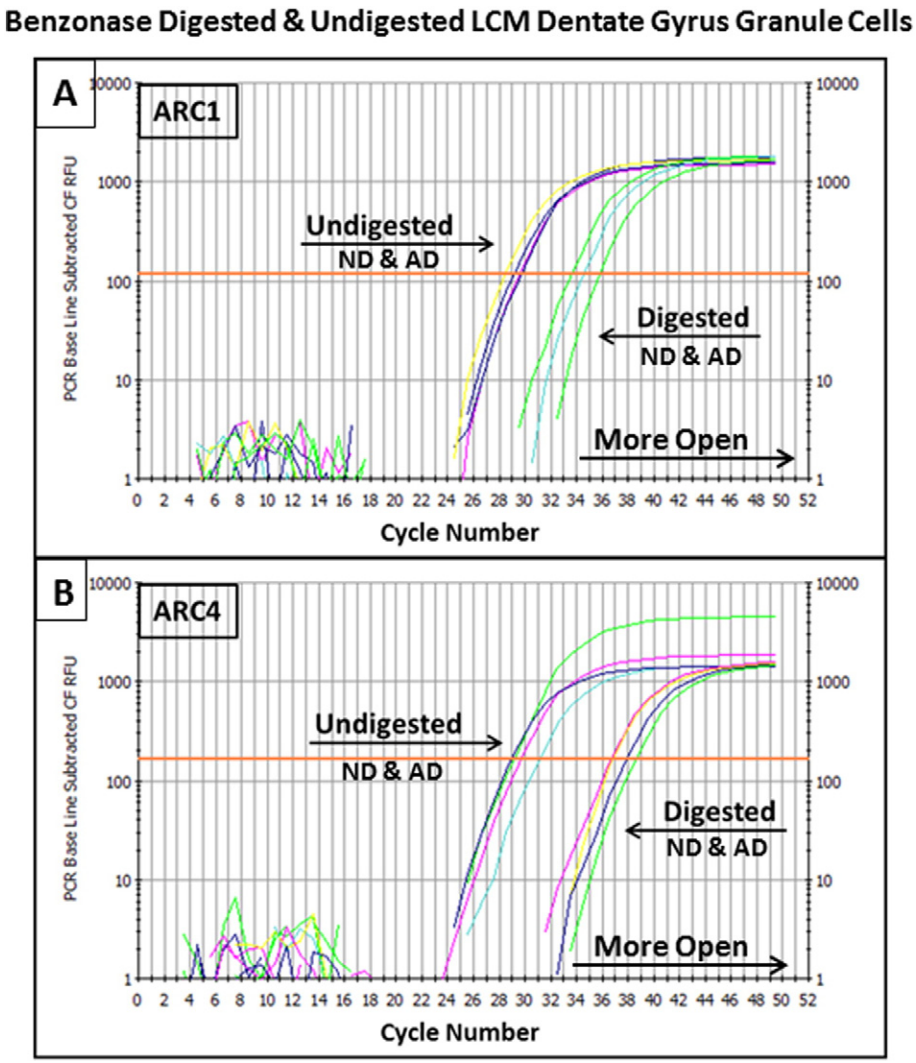

Fig. 4. Dentate gyrus granule cells from 5 ND and 5 AD cases were obtained via LCM and underwent Benzonase digestion and qPCR to determine relative openness of chromatin in 4 regions of the ARC gene. (A) Graph is representative of qPCR traces in the promoter region of Arc (ARC1) from 1 ND and 1 AD case. (B) Graph is representative of qPCR traces in an intronic region of Arc (ARC4) from 1 ND and 1 AD case. As predicted and seen in both A and B, undigested samples should have equivalent and lower C_T values than Benzonase-digested samples.

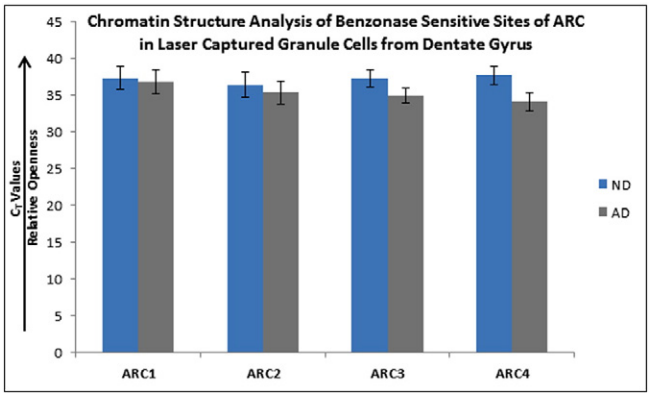

Fig. 5. Dentate gyrus granule cells from 5 ND and 5 AD cases were obtained via LCM and then underwent Benzonase digestion and qPCR. Four regions of the ARC gene were examined for chromatin accessibility. No significant difference was found between primer groups or in accessibility between ND and AD in any of the gene regions. Error bars signify SEM.

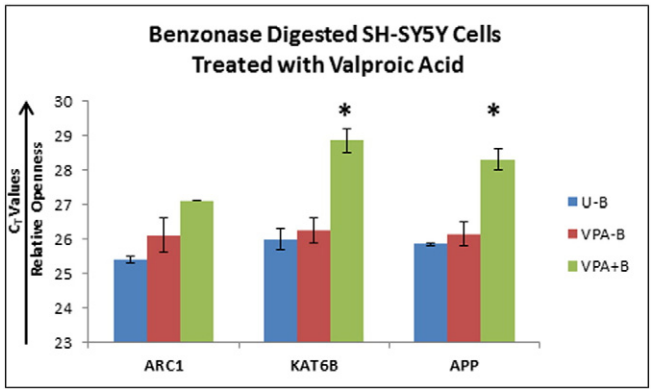

Fig. 7. To validate Benzonase efficacy, SH-SY5Y cells were treated with VPA, an agent known to relax chromatin, and then digested with Benzonase. qPCR results indicate that VPA relaxed the chromatin in the primer-specific areas of KAT6B and APP with significant difference in relative openness between VPA-treated cells with and without Benzonase digestion with Student t test of $P < .05$*. Abbreviations: U-B, untreated and no Benzonase digestion; VPA-B, VPA treated and no Benzonase digestion; VPA + B, VPA treated and Benzonase digested. Error bars signify SEM.

applicability of this method to examination of multiple genes as well as multiple sites within 1 gene. We have experimentally demonstrated the validity of our method by treating cells with valproate, a reagent known to render chromatin more permissive, and by comparison with DNase I digestion.

The premise behind our chromatin accessibility analysis using a nuclease and qPCR is that "open" chromatin will be subject to enzyme cleavage; therefore, less available to amplify in qPCR; leading to higher C_T values. Meaning, the higher the C_T value is, the more accessible the chromatin is for initiation of transcription. Our novel protocol uses Benzonase, a nuclease that can successfully digest chromatin and whose efficacy is not inhibited by actin, as is the case with DNase I (Lazarides and Lindberg, 1974).

Initial experiments in frozen brain homogenates from 1 AD case demonstrated differential chromatin "openness" between 2 brain regions, as well as between 2 genes of interest. In this case, the promoter region of KAT6B and APP appeared more open in MTG than in CBL. When the number of cases was increased to compare chromatin accessibility between brain regions and disease states, the results showed that defined regions of both genes were more open in AD than ND in both brain regions and that both genes are more open in MTG than CBL, confirming the previous study.

When we tested the lower limits of our protocol on 5 neurons obtained by LCM, we yielded seemingly different results than shown in the homogenates. We can speculate that cell heterogeneity in homogenates can mask the results that we may observe down to single-cell to few-cells level (Wills et al., 2013). Nevertheless, we emphasize that, without additional samples and replicates, we cannot draw a valid conclusion on chromatin accessibility from our 5 cell data.

We also used our method to examine chromatin structure at multiple sites within 1 gene. ARC was interrogated at 4 sites in MTG homogenate samples. Results showed that the promoter region of the ARC gene was significantly less open in AD than ND. When done on the dentate gyrus of LCM samples, there was no significant difference found in any of the 4 regions of the gene. We stress that this is a

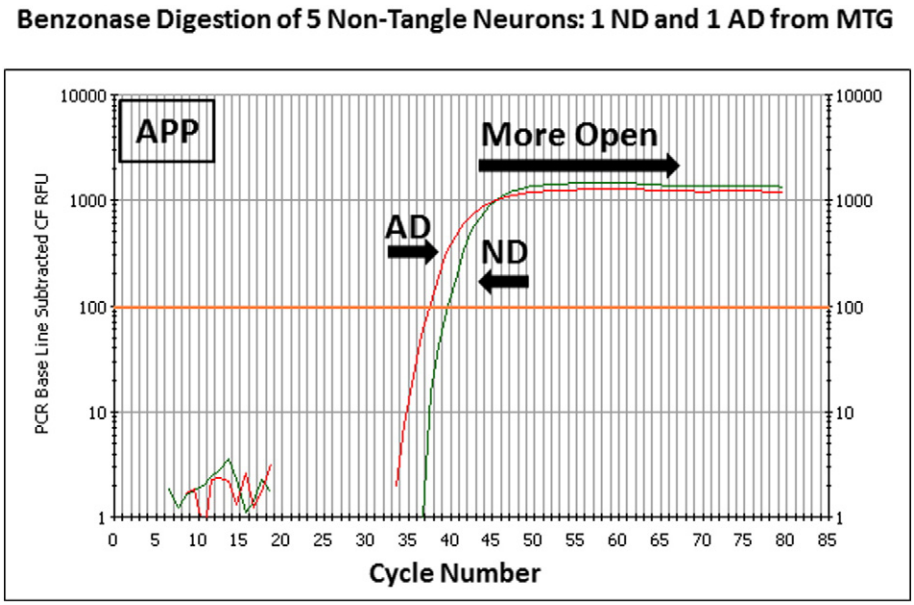

Fig. 6. Five cell equivalents of MTG layer 3 pyramidal neurons with no tangle pathology from 1 ND and 1 AD case were acquired via LCM and then underwent Benzonase digestion and qPCR to determine relative openness of chromatin in the promoter region of APP. qPCR traces show that the promoter region of APP appears to be more accessible in ND than in AD.

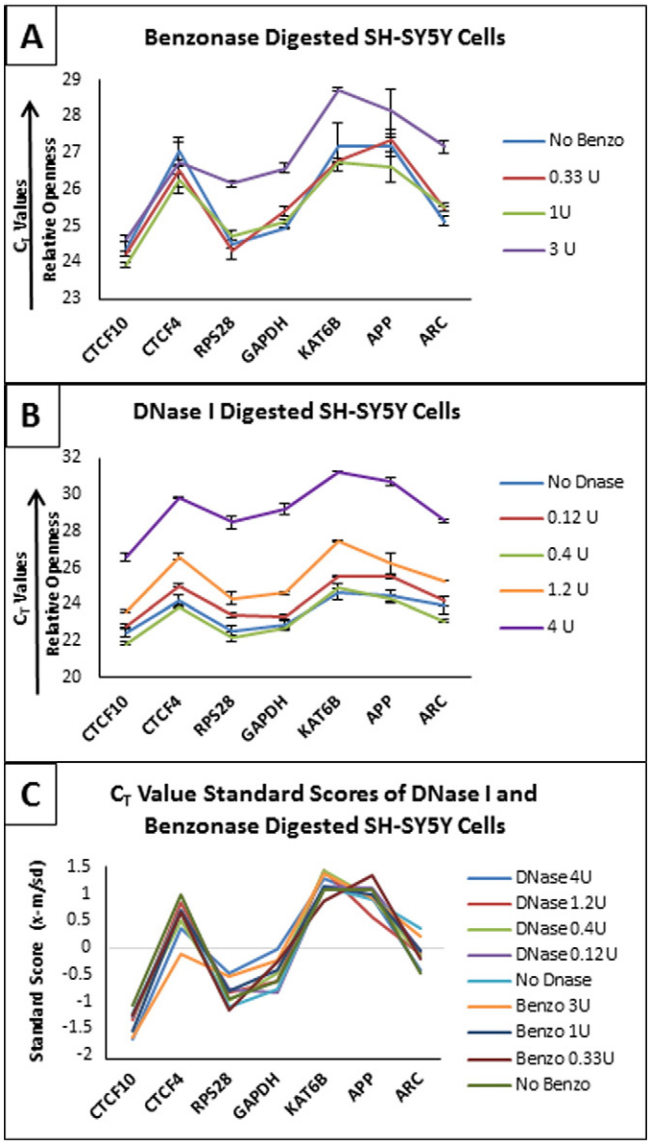

Fig. 8. To compare Benzonase to DNase I, SH-SY5Y cells were digested with various concentrations of Benzonase (A) or DNase I (B). qPCR indicated that Benzonase digestion exhibited similar patterns of relative openness to DNase I digestion in 7 distinct regions of the genome. (C) Standard scores (x-m/sd) of C_T data validate that DNase I and Benzonase are comparable under the conditions examined. Error bars signify SEM.

different brain region in which neurons do not typically show the neuron loss (West et al., 1994) or neurofibrillary tangle pathology of Alzheimer's disease. Therefore, the finding of no difference between AD and ND in this region is to be expected.

Validation experiments began with treating SH-SY5Y cell with VPA, an agent known to decondense chromatin (Marchion et al., 2005). The treatment relaxed the chromatin as expected, validated by showing that the chromatin in VPA-treated cells digested with Benzonase was more open than that in cells not digested. Finally, when comparing chromatin structure (accessibility) in SH-SY5Y cells that had been digested with Benzonase to those digested with DNase I, the criterion standard used for chromatin studies in cultured cells, similar patterns emerged. This concluding validation step demonstrates the efficacy and usefulness of Benzonase for chromatin structure analysis studies.

New methods to determine chromatin accessibility seem to arise at a consistent pace. One of the most recent examines chromatin structure at the single-cell level, however, only in cultured cells (Buenrostro et al., 2015). Up until now, no method existed to determine chromatin structure in frozen tissue samples at the level of defined cells. The protocol detailed here bridges that gap. This proposed novel method for frozen tissue demonstrates the capability to choose specific cell types to interrogate based on disease versus nondisease, or cells that express a particular protein, cells of a certain morphology, or cells in particular regions of tissue. This potential could translate into the ability to identify specific regulatory mechanisms implicated in disease or normal cellular processes.

Numerous epigenetic mechanisms converge to modulate chromatin structure, and many methods exist to delineate this structure. Most of these methods require considerable amounts of starting material, personnel time, reagent costs, and expensive equipment. The protocol we describe investigates chromatin structure at distinct genomic loci from frozen tissue and defined cells obtained by LCM. In addition, the protocol is rapid, inexpensive, and easily executed in a typical research laboratory setting.

Disclosure statement

The authors have no conflicts of interest to disclose.

Acknowledgements

The authors thank the Banner Sun Health Research Institute Brain and Body Donation Program of Sun City, AZ, for providing human brain samples. The Brain and Body Donation Program is supported by the National Institute of Neurological Disorders and Stroke (U24 NS072026, National Brain and Tissue Resource for Parkinson's Disease and Related Disorders), the National Institute on Aging (P30 AG19610, Arizona Alzheimer's Disease Core Center), the Arizona Department of Health Services (contract 211002, Arizona Alzheimer's Research Center), the Arizona Biomedical Research Commission (contracts 4001, 0011, 05-901, and 1001 to the Arizona Parkinson's Disease Consortium), and the Michael J. Fox Foundation for Parkinson's Research. This work was supported by NIH R01 AG036400 and AARC DHS Award FY 2012 to Paul D. Coleman.

References

Amatori, S., Ballarini, M., Faversani, A., Belloni, E., Fusar, F., Bosari, S., ... Fanelli, M., 2014. PAT-ChIP coupled with laser microdissection allows the study of chromatin in selected cell populations from paraffin-embedded patient samples. Epigenetics Chromatin 7 18–8935-7-18. eCollection 2014.

Buenrostro, J.D., Litzenburger, U.M., Ruff, D., Gonzales, M.L., Snyder, M.P., Chang, H.Y., Greenleaf, W.J., 2015. Single-cell chromatin accessibility reveals principles of regulatory variation. Nature 523 (7561), 486–490.

Chabbert, C.D., Adjalley, S.H., Klaus, B., Fritsch, E.S., Gupta, I., Pelechano, V., Steinmetz, L.M., 2015. A high-throughput ChIP-seq for large-scale chromatin studies. Mol. Syst. Biol. 11 (1), 777.

Chouliaras, L., Mastroeni, D., Delvaux, E., Grover, A., Kenis, G., Hof, P.R., ... van den Hove, Daniel L.A., 2013. Consistent decrease in global DNA methylation and hydroxymethylation in the hippocampus of Alzheimer's disease patients. Neurobiol. Aging 34 (9), 2091–2099.

Dekker, J., Rippe, K., Dekker, M., Kleckner, N., 2002. Capturing chromosome conformation. Science 295 (5558), 1306–1311.

Fanelli, M., Amatori, S., Barozzi, I., Soncini, M., Dal Zuffo, R., Bucci, G., ... Minucci, S., 2010. Pathology tissue-chromatin immunoprecipitation, coupled with high-throughput sequencing, allows the epigenetic profiling of patient samples. Proc. Natl. Acad. Sci. U. S. A. 107 (50), 21535–21540.

Fanelli, M., Amatori, S., Barozzi, I., Minucci, S., 2011. Chromatin immunoprecipitation and high-throughput sequencing from paraffin-embedded pathology tissue. Nat. Protoc. 6 (12), 1905–1919.

Felisbino, M.B., Tamashiro, W.M., Mello, M.L., 2011. Chromatin remodeling, cell proliferation and cell death in valproic acid-treated HeLa cells. PLoS One 6 (12), e29144.

Felisbino, M.B., Gatti, M.S., Mello, M.L., 2014. Changes in chromatin structure in NIH 3 T3 cells induced by valproic acid and trichostatin A. J. Cell. Biochem. 115 (11), 1937–1947.

Fullwood, M.J., Liu, M.H., Pan, Y.F., Liu, J., Xu, H., Mohamed, Y.B., ... Ruan, Y., 2009. An oestrogen-receptor-alpha–bound human chromatin interactome. Nature 462 (7269), 58–64.

Gilmour, D.S., Lis, J.T., 1984. Detecting protein-DNA interactions in vivo: distribution of RNA polymerase on specific bacterial genes. Proc. Natl. Acad. Sci. U. S. A. 81 (14), 4275–4279.
Gilmour, D.S., Lis, J.T., 1985. In vivo interactions of RNA polymerase II with genes of *Drosophila melanogaster*. Mol. Cell. Biol. 5 (8), 2009–2018.
Grøntved, L., Bandle, R., John, S., Baek, S., Chung, H.J., Liu, Y., ... Levens, D., 2012. Rapid genome-scale mapping of chromatin accessibility in tissue. Epigenetics Chromatin 5 (1) 10–8935-5-10.
Guzowski, J.F., Lyford, G.L., Stevenson, G.D., Houston, F.P., McGaugh, J.L., Worley, P.F., Barnes, C.A., 2000. Inhibition of activity-dependent arc protein expression in the rat hippocampus impairs maintenance of long-term potentiation and the consolidation of long-term memory. J. Neurosci. 20, 3993–4001.
Hao, H., Liu, H., Gonye, G., Schwaber, J.S., 2008. A fast carrier chromatin immunoprecipitation method applicable to microdissected tissue samples. J. Neurosci. Methods 172 (1), 38–42.
He, H.H., Meyer, C.A., Hu, S.S., Chen, M.W., Zang, C., Liu, Y., ... Brown, M., 2014. Refined DNase-seq protocol and data analysis reveals intrinsic bias in transcription factor footprint identification. Nat. Methods 11 (1), 73–78.
Hughes, J.R., Roberts, N., McGowan, S., Hay, D., Giannoulatou, E., Lynch, M., ... Higgs, D.R., 2014. Analysis of hundreds of cis-regulatory landscapes at high resolution in a single, high-throughput experiment. Nat. Genet. 46 (2), 205–212.
Jaenisch, R., Bird, A., 2003. Epigenetic regulation of gene expression: how the genome integrates intrinsic and environmental signals. Nat. Genet. 33, 245–254 Suppl.
Krebs, J.E., Peterson, C.L., 2000. Understanding "active" chromatin: a historical perspective of chromatin remodeling. Crit. Rev. Eukaryot. Gene Expr. 10 (1), 1–12.
Lazarides, E., Lindberg, U., 1974. Actin is the naturally occurring inhibitor of deoxyribonuclease I. Proc. Natl. Acad. Sci. U. S. A. 71 (12), 4742–4746.
Li, Y., Huang, W., Niu, L., Umbach, D.M., Covo, S., Li, L., 2013. Characterization of constitutive CTCF/cohesin loci: a possible role in establishing topological domains in mammalian genomes. BMC Genomics 14 553–2164-14-553.
Lupien, M., Eeckhoute, J., Meyer, C.A., Wang, Q., Zhang, Y., Li, W., ... Brown, M., 2008. FoxA1 translates epigenetic signatures into enhancer-driven lineage-specific transcription. Cell 132 (6), 958–970.
Marchion, D.C., Bicaku, E., Daud, A.I., Sullivan, D.M., Munster, P.N., 2005. Valproic acid alters chromatin structure by regulation of chromatin modulation proteins. Cancer Res. 65 (9), 3815–3822.
Mastroeni, D., Grover, A., Delvaux, E., Whiteside, C., Coleman, P.D., Rogers, J., 2011. Epigenetic mechanisms in Alzheimer's disease. Neurobiol. Aging 32 (7), 1161–1180.
Natarajan, A., Yardimci, G.G., Sheffield, N.C., Crawford, G.E., Ohler, U., 2012. Predicting cell-type-specific gene expression from regions of open chromatin. Genome Res. 22 (9), 1711–1722.
Orlando, V., 2000. Mapping chromosomal proteins in vivo by formaldehyde-cross-linked-chromatin immunoprecipitation. Trends Biochem. Sci. 25 (3), 99–104.
Quina, A.S., Buschbeck, M., Di Croce, L., 2006. Chromatin structure and epigenetics. Biochem. Pharmacol. 72 (11), 1563–1569.
Rao, S., Procko, E., Shannon, M.F., 2001. Chromatin remodeling, measured by a novel real-time polymerase chain reaction assay, across the proximal promoter region of the IL-2 gene. J. Immunol. 167 (8), 4494–4503.
Sexton, T., Kurukuti, S., Mitchell, J.A., Umlauf, D., Nagano, T., Fraser, P., 2012. Sensitive detection of chromatin coassociations using enhanced chromosome conformation capture on chip. Nat. Protoc. 7 (7), 1335–1350.
Sheffield, N., Furey, T., 2012. Identifying and characterizing regulatory sequences in the human genome with chromatin accessibility assays. Genes 3 (4), 651–670.
Sherrington, C., 1906. *The Integrative Action of the Nervous System*. CUP Archive.
Song, L., Crawford, G.E., 2010. DNase-seq: a high-resolution technique for mapping active gene regulatory elements across the genome from mammalian cells. Cold Spring Harb. Protoc. (2) 2010, pdb.prot5384.
Soulé, J., Alme, M., Myrum, C., Schubert, M., Kanhema, T., Bramham, C.R., 2012. Balancing arc synthesis, mRNA decay, and proteasomal degradation: maximal protein expression triggered by rapid eye movement sleep-like bursts of muscarinic cholinergic receptor stimulation. J. Biol. Chem. 287 (26), 22354–22366.
Su, Z., Boersma, M.D., Lee, J.H., Oliver, S.S., Liu, S., Garcia, B.A., Denu, J.M., 2014. ChIP-less analysis of chromatin states. Epigenetics Chromatin 7 7–8935-7-7. eCollection 2014.
Tewari, A.K., Yardimci, G.G., Shibata, Y., Sheffield, N.C., Song, L., Taylor, B.S., ... Febbo, P.G., 2012. Chromatin accessibility reveals insights into androgen receptor activation and transcriptional specificity. Genome Biol. 13 (10), R88.
Thurman, R.E., Rynes, E., Humbert, R., Vierstra, J., Maurano, M.T., Haugen, E., ... Stamatoyannopoulos, J.A., 2012. The accessible chromatin landscape of the human genome. Nature 489 (7414), 75–82.
Vatolin, S., Khan, S.N., Reu, F.J., 2012. Direct chromatin PCR (DC-PCR): hypotonic conditions allow differentiation of chromatin states during thermal cycling. PLoS One 7 (9), e44690.
West, M.J., Coleman, P.D., Flood, D.G., Troncoso, J.C., 1994. Differences in the pattern of hippocampal neuronal loss in normal ageing and Alzheimer's disease. Lancet 344, 769–772.
Wills, Q.F., Livak, K.J., Tipping, A.J., Enver, T., Goldson, A.J., Sexton, D.W., Holmes, C., 2013. Single-cell gene expression analysis reveals genetic associations masked in whole-tissue experiments. Nat. Biotechnol. 31 (8), 748–752.